Available online at www.sciencedirect.com
ScienceDirect
Desalination 246 (2009) 526–533
DESALINATION
www.elsevier.com/locate/desal

Hydrodynamically deposited $CaCO_3$ and $CaSO_4$ scales

Abdul Quddus*, Luai M. Al-Hadhrami
Research Institute, King Fahd University of Petroleum and Minerals, PO Box 1524, Dhahran 31261, Saudi Arabia
Tel. +966 (3) 860-3533; Fax +966 (3) 860-3996; email: amquddus@kfupm.edu.sa

Received 8 February 2007; Accepted 23 November 2008

Abstract

A laboratory study was carried out to explore the effect of solution hydrodynamics on the deposition of calcium carbonate scale on Stainless Steel 316 and calcium sulfate scale on aluminum substrates using a rotating cylinder electrode apparatus. The results of the study indicate a strong influence of solution hydrodynamics on the deposition rate of these scales. Furthermore, the analysis of the data obtained in the study shows a good agreement with the theoretical prediction of a diffusion controlled process. Morphological examinations of the deposited crystals conducted on the exposed specimens by scanning electron microscopy revealed a variety of crystal shapes comprising: dendrites, sand-rose, half-moon, rhombic, hexagonal or prismatic needles/rods like crystals growing at nucleating sites and branching out randomly over the substrates. Secondary growth on the already existing primary crystals was also identified.

Keywords: Scale; Calcium sulfate scale, Calcium carbonate scale; Rotating cylinder electrode; RCE, $CaSO_4$, $CaCO_3$

1. Introduction

The hard and adherent substances deposited from process fluids on various hot surfaces are termed as scaling/fouling. These deposits pose major problems for process industries worldwide because of unpredictable failures and frequent shutdown occurring because of scaling. The scale deposits reduce the thermal efficiency of the heat transfer equipment. Scale deposits in oil-producing wells, restrict flow through the tubing and drastically decrease oil production. The decrease in thermal efficiency and/or loss of production results in decline of revenues [1,2]. The synergistic effect of scale and corrosion is an important problem that the plant designers and operators have to constantly battle with throughout the whole life of the plant [3]. At relatively high scaling rates, the hydrodynamics of fluid flow can play a dominant role in the scale formation process. Therefore, basic understanding of scale formation is essential for effective control and a scale mitigation program.

*Corresponding author.

0011-9164/09/$– See front matter
doi:10.1016/j.desal.2008.11.005

To study scale deposition in the laboratory, generally, open- (once through type) or closed-flow loops (re-circulating type) [4–8] are employed to simulate actual practical situations encountered in industry. These experiments are laborious and time consuming usually requiring long periods of rigorous monitoring along with copious volumes of feed solution.

Alternatively, it is relatively easy to use rotating cylinder electrode (RCE) or rotating disk electrode (RDE) methods to study scale formation in the laboratory. These techniques are well-established methods for studying kinetics of corrosion [9–13] and electro-deposition [14,15]. These techniques have been utilized for the study of scale deposition [16–22] to a limited extent.

Neville et al. [19–21] studied the electrochemical aspects of surface/solution interactions in $CaCO_3$ scale initiation, growth and inhibition on a rotating disk electrode made from SS-316L at different rotational speeds. Their technique utilizes a well-known oxygen reduction electrochemical phenomenon at the RDE surface. They showed that the presence of scaling on the samples resulted in the reduction of electro-active surface area and the corresponding electrochemical response. They demonstrated a good correlation between the surface coverage predicted by the proposed electrochemical technique and that of the image analysis conducted on the surface of scaled and clean samples. The technique appears to be viable and promising in understanding the mechanism of scale formation, assessment of inhibitors and their interactions on the solid surface.

Utilizing the technique proposed by Neville [19–21], Chen et al. [22] investigated the $CaCO_3$ scale formation and adhesion by monitoring surface coverage of the specimens electrochemically by oxygen reduction at the RDE surface made from stainless steel under potentiostatic control in three different scale forming solutions. They found that the surface coverage depended on adhesion of scale on the specimens which in turn resulted in the reduction of electrochemical response (current) considerably whereas the bulk precipitation depended on the concentration of ions in the solution. They concluded that the bulk precipitation and adhesion on the surface are two different processes and depend on supersaturation indices of scale forming solutions.

The alkaline earth sulfates and carbonates including calcium sulfate, strontium sulfate, barium sulfate, and calcium carbonate are the most commonly found scales in oil production environments as was characterized by the analyses of actual scale samples obtained from the Arabian Gulf region by Singh et al. [23].

In earlier works [16–18], we studied the deposition of strontium sulfate, barium sulfate and calcium sulfate scales by using a rotating cylinder electrode made from SS-316 at various rotational speeds. The present work further reports our results developed in this study on calcium carbonate and calcium sulfate scales that were hydrodynamically deposited on AISI SS-316 and commercial-grade aluminum specimens utilizing RCE equipment.

2. Experimental procedure

The schematic of an EG&G Princeton Applied Research rotating cylinder electrode equipment, test cell and experimental set-up used in the study are shown in Fig. 1. Full details of the experimental procedure, improvisation of the glass cell and other information can be found elsewhere [17,18].

The analytical reagents $CaCl_2$, Na_2SO_4, and Na_2CO_3 were dissolved in deionized water to produce $CaSO_4$ and $CaCO_3$ scales by coprecipitation. Gravity-assisted solution replenishment at a rate of 1 to 1.5 L/h to the cell was made to ensure constant availability of scale forming species to the electrode surface. All experiments were conducted at 60°C temperature and atmospheric pressure for 6 h duration at various preset rotational speeds (rpm).

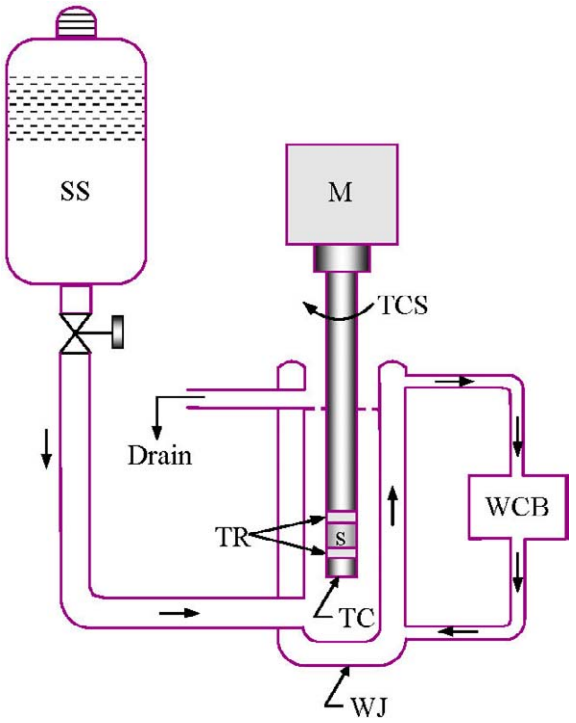

Fig. 1. Schematic of the experimental set-up of rotating cylinder electrode equipment. M, motor to rotate specimen at a preset rpm; TCS, Teflon-coated shaft. TR, Teflon ring; S, Cylindrical specimen; TC, Teflon cap; WJ, Hot water jacket; WCB, Hot water circulation bath; SS, Supersaturated solution.

An analytical laboratory balance with an accuracy of ±0.1 mg was used to measure the weight gain of scaled specimens after oven drying.

The error analysis of the data developed in the study was accomplished by Engineering Equation Solver (EES) computer software. The method for calculating and performing the uncertainty and error analyses was previously outlined [24].

The morphology of calcium carbonate and calcium sulfate crystals was studied by using flat coupons having dimensions of 20 mm by 8 mm by 1.5 mm. The coupons were polished to 600 grit with silicon carbide (SiC) paper. After polishing, they were thoroughly degreased with acetone and rinsed with distilled water. Duplicate specimens were assembled in a Teflon holder that was placed in the test cell where they were exposed to the scale-forming solutions for 1 to 6 h.

After the tests, the coupons were retrieved, rinsed with distilled water, dried in an oven and preserved for scanning electron microscopy (SEM) examination to study the morphology of the hydrodynamically deposited crystals on the substrate surface.

3. Results and discussion

The surface roughness texture of both 600 grit polished SS-316 and aluminum specimens was measured by a Bendix linear profiling system, Model 5054. The average surface roughness (Ra) value obtained for SS-316 was 55 μ inch while it was 82.5 μ inch for aluminum. Aluminum, a soft material, showed a comparatively higher value of surface roughness than SS-316.

To produce $CaCO_3$ scale we used $CaCl_2$ and Na_2CO_3 salts both at a rate of 0.0008 moles/L. Thus, 0.888 g of $CaCl_2$ and 0.848 g of Na_2CO_3 were dissolved in deionized water to make 10 L of total $CaCO_3$ scale-forming solution for an experimental run. Similarly, for $CaSO_4$ scale, $CaCl_2$ and Na_2SO_4 were used at a constant concentration of 0.03 moles/L. Hence, 33.297 g of $CaCl_2$ and 42.612 g of Na_2SO_4 were utilized to make 10 L of $CaSO_4$ scale-forming solution.

An induction period of around 50 min was determined experimentally (deposition vs. time) at fixed RPM of 500 for the $CaSO_4$ scale, while for the $CaCO_3$ scale it was taken from an earlier work [6] as about 70 min that was obtained under similar solution concentration and surface finish. The effective exposure duration during which the measurable weight gain obtained by the analytical balance was determined as the experiment time minus the induction period. Therefore, the scaling rates were calculated by dividing the weight of scale obtained per unit area by the effective exposure duration.

The deposition of sparingly soluble $CaCO_3$ and $CaSO_4$ salts on Stainless Steel 316 and

aluminum substrates was studied using a rotating cylinder electrode system under simulated fluid flow conditions at various preset rotational speeds. The increase in the speed of rotation of specimens, as well as mixing of solution, had a strong impact on the rate of mass transport of $CaCO_3$ and $CaSO_4$ scales to the electrode surface where they were adsorbed and finally deposited on the surface of the specimens. This process of adhesion of scale on the surface yielded a measurable weight gain of RCE samples due to scale formation.

An overall uncertainty error of ±12% in the scale deposition rate data generated in the study was indicated by the Engineering Equation Solver (EES) software. Further analysis of the data was carried out to demonstrate the effect of solution hydrodynamics at various Reynolds numbers that were obtained corresponding to each selected rotational speed using the procedure suggested by Gabe [13] on the rate of deposition of calcium carbonate and sulfate scales on the specimens.

The data thus developed in the present work are summarized in Tables 1 and 2 for each type of scale studied. The effect of the increasing Reynolds number on the deposition rate of calcium carbonate and sulfate scales is shown in Figs. 2 and 3. The results show that the deposition rate increases linearly with the increase in the Reynolds number as $(Re)^{0.5}$ for these scales deposited on the aluminum and SS-316 substrates. The results are in agreement with earlier studies [7,8, 17,18].

The $CaCl_2$, Na_2SO_4 and Na_2CO_3 reagents are ionic compounds. Because we used a supersaturated solution prepared from these salts, two process were obvious upon mixing. These are: firstly, precipitation of scale in the bulk of solution due to chemical reaction between the commingling species, and secondly, the adhesion of scale on the surface. The precipitation will continue as long as the ionic strength (active ions–chemical potential) of solution is available but the adherence of the scale on the surface of the sample depends on the surface binding energy or activation/free energy of the metal. If the metal has more affinity for the precipitated scale present in the bulk of the solution, it will attract it more and eventually result in increased deposition or mass gain on the specimen(s). Therefore, the solution replenishment arrangement adopted

Table 1
Effect of Reynolds number on the deposition rate of $CaCO_3$ scale on Stainless Steel 316 (conc. = 0.0008 mole/L, temp.= 60 °C, effective time = 4 h and 50 min)

Serial no.	rpm	Equivalent Reynolds number		$CaCO_3$ scale deposition rate ($g.m^{-2}.h^{-1}$)
		Re	$(Re)^{1/2}$	SS 316
1	100	1,457	38.171	1.392
2	250	3,642	60.349	2.052
3	500	7,284	85.346	2.895
4	1000	14,567	120.694	4.262
5	1500	21,851	147.821	4.944
6	2000	29,135	170.690	6.127
7	2500	36,418	190.835	6.916
8	3000	43,702	200.050	7.431

Table 2
Effect of Reynolds number on the deposition rate of $CaSO_4$ scale on aluminum (conc.= 0.03 mole/L, temp.= 60 °C, effective time = 5 h and 10 min)

Serial no.	rpm	Equivalent Reynolds number		$CaSO_4$ scale deposition rate ($g.m^{-2}.h^{-1}$)
		Re	$(Re)^{1/2}$	Aluminum
1	100	1,457	38.171	15.805
2	250	3,642	60.349	34.267
3	500	7,284	85.346	46.730
4	750	10,928	104.537	58.106
5	1000	14,567	120.694	70.986
6	1250	18,213	134.956	74.161
7	1500	21,851	147.821	95.215
8	1750	25,498	159.681	75.783
9	2000	29,135	170.690	91.225

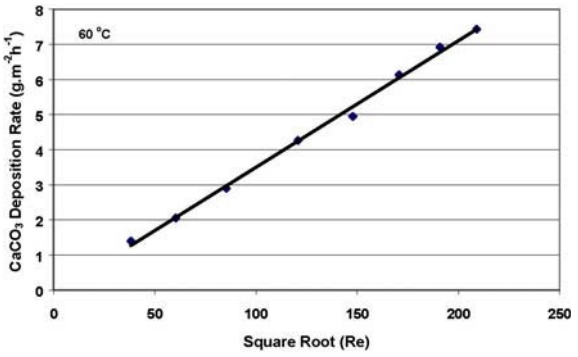

Fig. 2. Deposition rate of $CaCO_3$ on SS-316 as a function of $(Re)^{1/2}$.

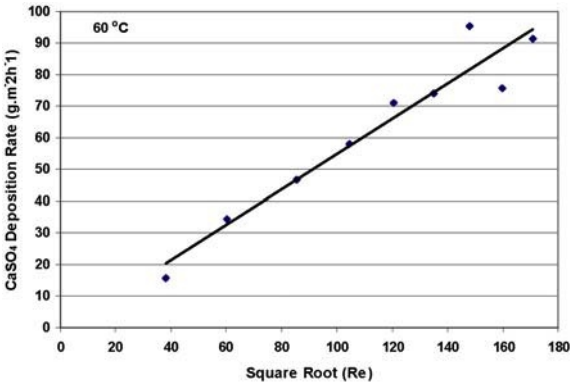

Fig. 3. Deposition rate of $CaSO_4$ on aluminum as a function of $(Re)^{1/2}$.

during the present work provided constantly the required chemical potential for the formation of scale from the solution.

We observed that the $CaCO_3$ scale was compact and strongly adhering onto the SS-316 specimens, whilst the $CaSO_4$ scale was comparatively loosely adhering to the surface of the aluminum and was fluffy as compared to the adherence of $CaCO_3$ scale on the stainless steel surface. Also the weight gain of $CaCO_3$ scale on stainless steel specimens was less compared to $CaSO_4$ scale on aluminum specimens (Tables 1 and 2). The disparity is due to the difference in their solubilities and therefore the concentrations used. It is to be noted that the solubility of $CaSO_4$ is higher than solubility of $CaCO_3$ [1].

Owing to the fluffy and loose adherence nature of $CaSO_4$ scale (and its needle/rod-like growth mechanism; see Morphology section), the current experiments for $CaSO_4$ were limited up to 2000 rpm because breaking away of crystals/scale was noticed at higher RPMs (i.e., those greater than 2000). In addition, the weight gain of $CaSO_4$ scale obtained on aluminum is higher compared to its weight gain on SS-316 [18] under identical test conditions, which may be ascribed to the greater affinity of aluminum toward $CaSO_4$ scale than SS-316.

The present scale deposition results were obtained in the case of pure salts without any external seeding or contamination. Seeding is usually used to enhance the scale formation process [25]. However, the presence of impurities such as particulate matters, mixed salts, corrosion products and biological mass, as well as surface geometry and flow velocity, have significant influence on the deposition behavior of scale on the surface. The conjoint effect of these factors may affect the overall growth rate of scale, and under such conditions, the scaling/fouling rate may be linear, a falling rate or asymptotic as presented by Knudsen [26,27]. The asymptotic behavior of scaling/fouling of heat exchange equipment is observable when the rate of deposition and the rate of removal of scale is balanced by the flowing fluid.

3.1. Diffusional mass transport

The rigorous mixing of a scale-forming solution demonstrated a strong effect on the rate of mass transport of $CaCO_3$ and $CaSO_4$ scales to the electrode surface where it finally deposited on the surface of the specimens. The present data (Figs. 2 and 3) show that the $CaCO_3$ and $CaSO_4$ scaling rate increases with $(Re)^{0.5}$, suggesting further that the process is diffusion controlled. According to Levich's analysis [28], the mass transfer coefficient should increase with $(Re)^{0.5}$. If so, the plot of {log (scale)} vs. {log(Reynolds

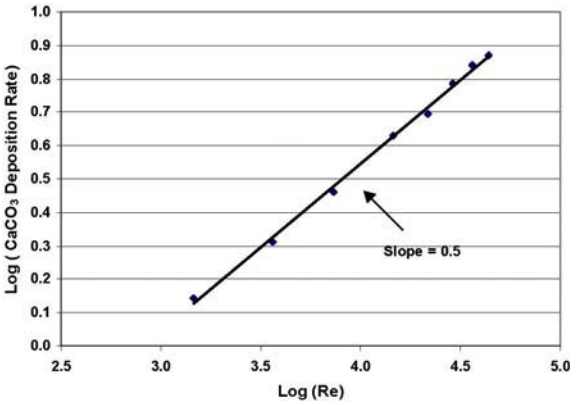

Fig. 4. Log-log plot of deposition rate vs. Reynolds number for $CaCO_3$ on SS-316.

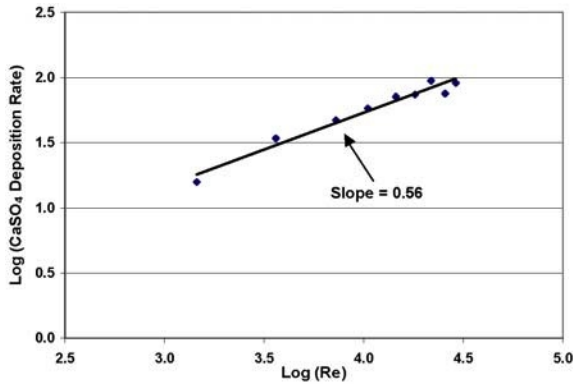

Fig. 5. Log-log plot of deposition rate vs. Reynolds number for $CaSO_4$ on aluminum.

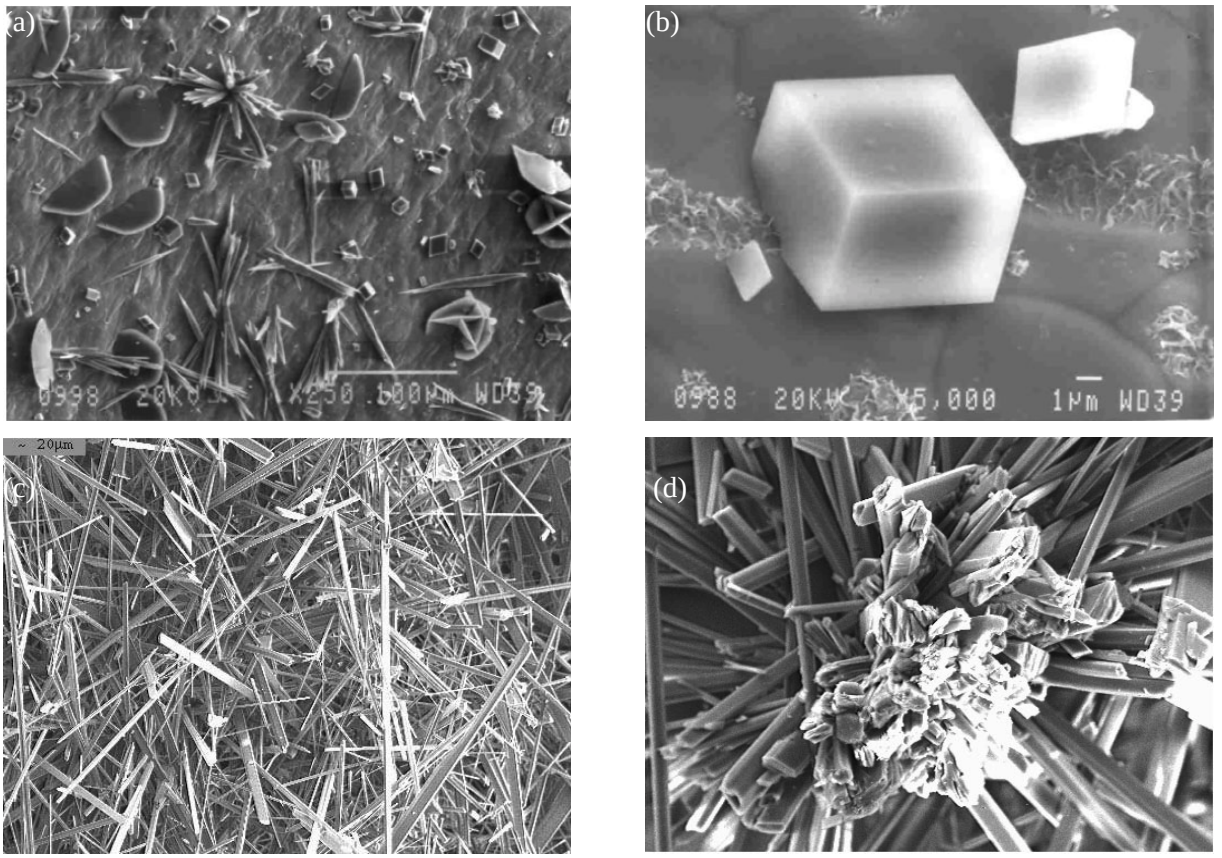

Fig. 6. SEM micrographs showing general morphology of $CaCO_3$ crystals on SS-316 (a,b) and $CaSO_4$ crystals on aluminum (c,d) substrates. (a) $CaCO_3$ crystals: rhombic/hexagonal, half-moon, sand-rose, flower and prismatic needles/rods, (b) $CaCO_3$ crystals rhombic/hexagonal (close-up), (c) $CaSO_4$ crystals: prismatic needles/rods, (d) $CaSO_4$ crystals: prismatic needles/rods with perpendicular growth (close-up).

No.)} should give a straight line with a theoretical slope of 0.5.

We plotted log(deposition rate) vs. log (Reynolds number) for the data generated during the current study. A straight line behavior is depicted in Figs. 4 and 5 having slopes of 0.5 for $CaCO_3$ scale on SS-316 and 0.56 for $CaSO_4$ scale on aluminum, respectively. These slopes are in agreement with the theoretically predicted value of 0.5 [28]. Hence, the present work demonstrates and supports the diffusion controlled aspect of the scale deposition process.

3.2. Morphology

The SEM examinations of $CaCO_3$ and $CaSO_4$ scales, in general, exhibited a wide variety of structural shapes of crystals consisting of dendrite flower shape, sand-rose shape, half-moon shape, rhombic, hexagonal, prismatic needle/rod or plate-like growth. Plate-like or flat crystals perhaps had been formed due to the coagulation of prismatic rods, which then finally acquired sand-rose and half-moon shapes upon conglomeration. It was also observed during the examination that the growth of $CaCO_3$ and $CaSO_4$ crystals initially started at the nucleation sites on the substrate surface and/or on the existing crystals and then branched out randomly in all directions.

Fig. 6 presents some typical morphological results of calcium carbonate and sulfate crystals deposited on SS-316 and aluminum substrates. The photomicrograph (Fig. 6a and b) shows prismatic needles/rods, half-moon, sand-rose, rhombic/hexagonal and flower shaped $CaCO_3$ crystals on the surface of the SS-316 substrate. Fig. 6c and 6d further present the morphology of $CaSO_4$ scale, showing needle- and rhombic-shaped crystals. Similar morphological results were obtained in earlier studies for $SrSO_4$ [4], $BaSO_4$ [17] and $CaSO_4$ [18] scale formation. The micrographs however, further indicate the random growth of secondary crystals emanating from the already deposited primary crystals. The subsequent crystals seem to have been growing at preferential nucleation sites available on the substrate or previously deposited scale crystals/layer. The reason seems to be a random growth of the subsequent crystallites in all directions on the previously deposited scale crystals, i.e., a sort of epitaxial growth, as revealed from the SEM photomicrographs (Fig. 6), which in turn, promotes the scale deposition process. In addition, the perpendicular growth of $CaCO_3$ as well as $CaSO_4$ crystals is also evident from these micrographs. It is conjectured that these typical microscopic structural shapes of $CaCO_3$ and $CaSO_4$ crystals can be attributable to the hydrodynamic effect of solution on micro-levels.

4. Conclusions

The data developed in the present study demonstrate the significant role of solution hydrodynamics on the scale deposition process. The turbulent mixing generated due to the agitation of the solution may be a major hydrodynamic factor that promotes scale formation. This is because the more active scale-forming species are adsorbed on the surface which ultimately adhere and deposit on the substrate. In addition, it also provides the necessary activation/surface energy that is manifested for the nucleation and/or epitaxial growth of scale crystals. Furthermore, this suggests that in order to control the excessive scale build-up, avoidance of turbulence must be exercised. Therefore, the hydrodynamic factor must be a part and parcel of any scale prognostic and control model.

The effect of rotational speed (fluid velocity) on calcium carbonate and calcium sulfate scales has been investigated in a rotating cylinder electrode device, at atmospheric pressure and at 60 °C. Within the range of experimental parameters explored during the present work for the deposition of $CaCO_3$ and $CaSO_4$ scales resulting from co-precipitation of pure salts, the following conclusions have been made:

- The solution hydrodynamics has a significant role in scale deposition process; therefore, it must be included in any scale prediction model or water treatment program for scale mitigation and control.
- A linear trend has been observed in the scale deposition rate verses $(Re)^{0.5}$ in the present work; however, in industrial situations, the deposition may result in different behavior, e.g., non-linear, asymptotic, etc.
- Analysis of the scale deposition data developed in the present work supports the well-established theoretical prediction of a diffusion controlled process.
- In the case of $CaSO_4$ formation, stainless steel 316 attracted less scale than aluminum under identical test parameters.
- The SEM examination of $CaCO_3$ and $CaSO_4$ scales revealed a variety of crystal shapes comprising needles, prismatic rods, rhombic, hexagonal, dendrites, sand-rose and half-moon plates. In addition, the random and epitaxial growth of secondary crystals on the primary crystals was also observed.

Acknowledgments

The support of the Research Institute of King Fahd University of Petroleum and Minerals for this work is gratefully acknowledged.

References

[1] D.E. Potts, R.C. Ahlert and S.S. Wang, Desalination, 36 (1981) 235–264.
[2] J.C. Cowan and D.J. Weintritt, eds., Water Formed Scale Deposits, Gulf Publishing, Houston, 1976.
[3] M. Al-Ahmed and F.A. Aleem, Desalination, 93 (1993) 287–310.
[4] M.I. Khokhar, S.K. Somuah, M.O. Amabeoku, I.M. Allam and A. Quddus, Proc. 4th Middle East Corrosion Conference, Bahrain, 1988, Part I, pp. 244–258.
[5] S.M. Zubair, A.K. Sheikh, M.O. Budair, M.U. Haq, A. Quddus and O.A. Ashiru, J. Heat Transfer (Trans. ASME), 119 (1997) 581–588.
[6] M.O. Budair, M.S. Sultan, S.M. Zubair, A.K. Skiekh and A. Quddus, J. Heat Mass Transfer, 34 (1998) 163–170.
[7] D. Hasson, M. Avriel, W. Resnick, T. Rosenman and S Windreich, I EC Fund., 7(1) (1968) 59–65.
[8] D. Hasson and J. Zahavi, I EC Fund., 9(1) (1970) 1–10.
[9] G. Liu, D.A. Tree and M.S. High, Corrosion, 50 (1994) 584–593.
[10] K.D. Efrid, E.J. Wright, J.A. Boros, and T.G. Hailey, Corrosion, 49 (1993) 992-1003.
[11] D.C. Silverman, Corrosion, 40 (1984) 220–226.
[12] D.C. Silverman, Corrosion, 44 (1988) 42–49.
[13] D.R. Gabe, J. Appl. Electrochem., 4 (1974) 91–108.
[14] O.A. Ashiru and J.P.G. Farr, J. Electrochem. Soc., 139(10) (1992) 2806–2810.
[15] C.T.J. Low, C.P. de Leon and F.C. Walsh, Aust. J. Chem., 58 (2005) 246–262.
[16] M.I. Khokhar, A. Quddus, I.M. Allam and T.A. Abbasi, Proc., 6th Middle East Corrosion Conference, Bahrain, 1994, Vol. 2, pp. 759–769.
[17] A. Quddus, and I.M. Allam, Desalination, 127 (2000) 127–131.
[18] A. Quddus, Desalination, 127 (2002) 57–63.
[19] A. Neville, A.P. Morizot and T. Hodgkiess, Mat. Perf., 37(5) (1998) 50–57.
[20] A. Neville, A.P. Morizot and T. Hodgkiess, J. Appl. Electrochem., 37(4) (1999) 455–462.
[21] A. Neville and A.P. Morizot, J. Crystal Growth, 243 (2002) 490–502.
[22] T. Chen, A. Neville and M. Yuan, J. Petrol. Sci. Eng., 46 (2005) 185–194.
[23] R.P. Singh and N.M. Abbas, Proc., 5th Middle East Corrosion Conference, Bahrain, 1991, Vol. 4, pp. 561–569.
[24] B.N. Taylor and C.E. Kuyatt, Guidelines for evaluating and expressing the uncertainty of NIST measurement results, National Institute of Standards and Technology, 1994, p. 1297.
[25] S.-T. Liu and G.H. Nancollas, J. Crystal Growth, 6 (1970) 281–289.
[26] J.G. Knudsen, Proc., 20th ASME/AIChE Heat Transfer Conference, 17 (1981) 29–38.
[27] G.F. Hewitt, ed., Hemisphere Handbook of Heat Exchanger Design, Hemisphere Publishing, New York, 1990, Section 3.17.
[28] V.G. Levich, Physicochemical Hydrodynamics, Prentice-Hall, Englewood Cliff, NJ, 1962.